Growth Pathway of Pt Clusters on α-Al_2O_3(0001) Surface

Chenggang Zhou,[†,‡] Jinping Wu,[‡] T. J. Dhilip Kumar,[†] Naduvalath Balakrishnan,*[,†] Robert C. Forrey,[§] and Hansong Cheng[||]

Department of Chemistry, University of Nevada Las Vegas, Las Vegas, Nevada 89154, Institute of Theoretical Chemistry and Computational Materials Science, China University of Geosciences Wuhan, Wuhan, China 430074, Department of Physics, Penn State University, Berks Campus, Reading, Pennsylvania 19610, and Air Products and Chemicals Inc., 7201 Hamilton Boulevard, Allentown, Pennsylvania 18195

Received: April 23, 2007; In Final Form: July 2, 2007

We report first-principles density functional theory calculations of the interaction between platinum subnanoclusters and the α-Al_2O_3(0001) surface. Energetically the most favorable adsorption sites were identified and substantial structural relaxation upon adsorption was observed. The optimized adsorption structures and the calculated average adsorption and adhesion energies were found to be size dependent. Results show that the clusters can be stably anchored on the surface with the driving force arising from the charge transfer from Pt atoms to O atoms of the substrate. Calculations of Pt atom agglomeration vs wetting suggest that metal clustering is strongly preferred.

I. Introduction

Oxide supported transition metal catalysts are used in a wide variety of heterogeneous catalytic processes such as hydrogenation/dehydrogenation and noxious pollutants reduction. In a typical heterogeneous catalytic system, nanoparticles of metal catalysts are dispersed on oxide surfaces such as alumina (Al_2O_3), zirconia (ZrO_2), MgO, and ceria (CeO_2).[1−9] It has been widely recognized that reactions often occur at the sharp corners, edges, and defect sites of catalyst surfaces and that the catalytic performance is largely dependent on the catalyst surface area, which is determined not only by the size of the catalyst particles but also by how strong the particles are anchored or dispersed on support materials.[10] It is known that a weak anchoring force would result in particle agglomeration, leading to shrinkage of catalyst surface area and decrease of catalytic efficiency.

One of the most important industrial catalysts is alumina-supported platinum, which has been utilized to catalyze a large variety of chemical reactions.[11−27] In general, platinum catalysts allow many chemical processes to occur at moderate conditions and alumina possesses superior mechanical and thermal stability.[28,29] Recent scanning tunneling microscopy studies by Sartale et al.[30] on growth of Pt nanoclusters on the Al_2O_3/NiAl(100) substrate revealed that the nanoclusters are mostly randomly distributed on surfaces, with a few exceptions in which some nanoparticles on surfaces are aligned. Theoretically, the catalytic systems are usually represented with a few extremely thin layers, often monolayer, of platinum on the support.[8] Using small Pt clusters on exceedingly small surface unit cells of supports, the interaction between catalysts and support materials was calculated in several theoretical studies.[16,21,25] It is expected that chemical reactivity of molecular species on the thin layers of catalytic systems would be considerably different from the ones with higher catalyst loading on the same support due to the support effects. Indeed, theoretical studies showed that in the case of low catalyst loading electron transfer from platinum to the substrate occurs and catalytic activity changes accordingly. In the case of high loadings, the catalysts are often modeled with crystalline surfaces without support because the effects of support on catalytic activity are deemed negligible. Nevertheless, regardless of catalyst loading, understanding of the interaction between catalyst and support is of fundamental importance. Indeed, even in the case of high loading, a weak catalyst−support interaction will eventually lead to catalyst segregation and a shortened catalyst life cycle.

Platinum nanoparticles have received much attention due to their superior catalytic activities. The activity of a catalyst to a specific reaction is largely dictated by the local electronic environments of the catalyst. Pure transition metal nanoparticles or clusters generate significant charge localization compared to their bulk crystal surfaces.[31] The active components of dispersed metal catalysts are small clusters, and therefore the cluster properties are responsible for the observed characteristics.[32] Dai et al.[33] have calculated the electronic structures of Pt_4 clusters using complete active space multiconfiguration self-consistent field (CAS-MCSCF) followed by multireference configuration interaction computations employing relativistic effective core potentials (RECPs) for Pt atoms. Xiao and Wang[34] studied both planar and three-dimensional Pt clusters, and their results show that planar Pt clusters of up to nine atoms are as stable as their three-dimensional isomers. In more recent work they reported[35] a density functional theory (DFT) study of methane activation reaction on Pt atoms and Pt_4 clusters. However, the interaction between Pt clusters and support materials has received much less theoretical attention.

In a previous study, we investigated the growth patterns of small Pt_n ($n = 2-15$) nanoclusters using the DFT method and identified energetically the most stable isomers.[36] In this paper, we present a systematic study using the DFT method to understand the adhesion of small Pt_n clusters for n up to 5 on

* Corresponding author. E-mail: naduvala@unlv.nevada.edu.
[†] University of Nevada Las Vegas.
[‡] China University of Geosciences Wuhan.
[§] Penn State University.
[||] Air Products and Chemicals Inc.

10.1021/jp073131w CCC: $37.00
Published on Web 08/23/2007

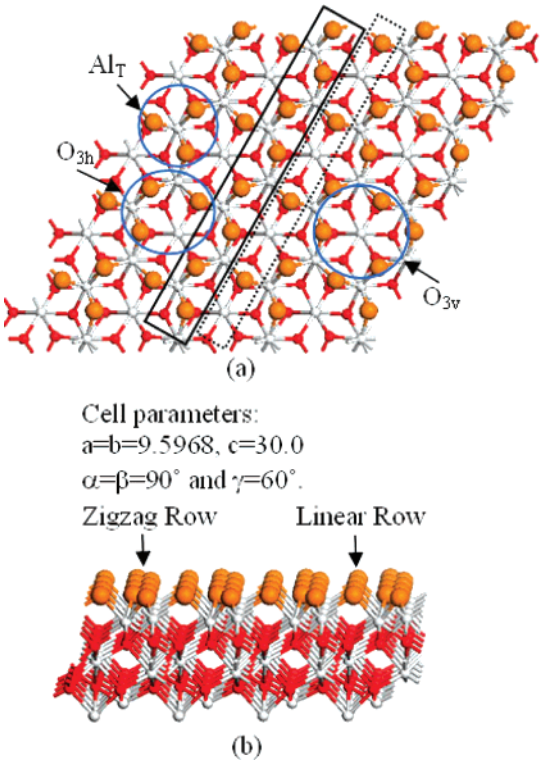

Figure 1. Structure of α-Al_2O_3(0001) surface. White balls represent aluminum and the red balls represent oxygen, while the top O layer is highlighted with larger orange balls. (a) Top view. The black box highlights the zigzag row, and the dashed box shows the linear row. (b) Side view.

the α-Al_2O_3(0001) surface. We chose only the highest binding energy clusters or isomers obtained in the previous study and place them on the reconstructed α-Al_2O_3(0001) surface. Unlike previous computational studies,[16,21,25] we chose a relatively larger surface unit cell that could accommodate various sizes of Pt clusters, which minimizes the lateral interaction between Pt clusters and yields information only on the interaction between the catalyst and the support substrate. It is understood that the present model does not represent a realistic catalytic system. However, the model allows us to obtain useful physical insights into the interaction between small Pt clusters and α-Al_2O_3 support. The relatively large support surface also allows us to systematically examine the effect of increased size of Pt clusters on the substrate to gain understanding of adhesion via platinum loading. In particular, we attempt to address whether the Pt atoms prefer agglomeration or wetting upon deposition on the substrate.

II. Theoretical Model and Computational Method

The present study employs a slab model to represent the α-Al_2O_3(0001) surface with the selected supercell duplicated by 2 × 2 from the primitive unit cell. The supercell comprises six layers of the substrate containing 24 Al atoms and 36 O atoms. The (0001) surface orientation alternates with Al and O layers with the top layer comprised only by O atoms and the bottom layer terminated by Al atoms. The minimum distance between adjacent slabs in all cases was set to 23 Å to minimize the interaction between slabs. The supercell parameters used in our calculations as well as the structure of the α-Al_2O_3(0001) surface are displayed in Figure 1. Each Al atom is covalently bonded with six O atoms, except for the bottom layer, at which the Al atom connects with only three O atoms. Likewise, each O atom forms a bond with four neighboring Al atoms with an exception at the top layer, for which an O atom connects with only two Al atoms in the second layer. A similar surface model with a smaller supercell has been used in previous calculations.[16,21] Several studies have suggested that the alumina surfaces are usually hydroxylated under typical experimental conditions.[37−39] However, little information is available on the detailed surface structure. To simplify the computation, we assume that the environment in which the Pt clusters are deposited on the substrate is water-free.

As shown in Figure 1a, two types of oxygen atoms can be identified in the top layer: atoms forming a zigzag pattern shown in the box with the solid black line and atoms aligned linearly between two zigzag rows shown in the black dashed box. The oxygen atoms also form three types of triangles on the surface as highlighted with circles in Figure 1a. This surface structural arrangement gives rise to multiple adsorption sites for Pt clusters. However, our numerical studies suggest that only three adsorption sites are energetically the most favorable: Al atop site (Al_T), O3 hollow site (O_{3h}), and O3 vacuum sites (O_{3v}). We will therefore only discuss adsorption of Pt clusters at these sites. The Al atop site is formed by two zigzag O atoms and one linear O atom attached to a single Al atom, which is a slightly distorted equilateral triangle with the O−O bond distances in the range of 2.34−2.66 Å. The O3 hollow site is formed by two zigzag O atoms and one linear O atom but supported by two different Al atoms with O−O bond lengths of 2.34, 2.66, and 3.47 Å, respectively. The O3 vacuum site is surrounded by a linear O atom and two O atoms from adjacent zigzag rows, which form an equilateral triangle with the O−O distance of 3.46 Å. Pt clusters up to $n = 5$ were then placed on the selected unit cell at these adsorption sites. In addition, we also examined the adhesion of a Pt monolayer as well as an aggregated Pt monolayer on the substrate. Possible binding sites of the clusters at the three adsorption sites were sampled to obtain the energetically most favorable configurations.

All the electronic structure calculations were done with density functional theory method under the generalized gradient approximation (GGA) with the exchange-correlation functional proposed by Perdew and Wang (PW91) as implemented in the VASP code.[40−43] The projector augmented wave pseudopotentials[44,45] were employed to describe the core electrons, and the valence electronic states are represented with a plane-wave basis set with a kinetic energy cutoff of 400 eV. A spin-polarization scheme was utilized to deal with the electronically open-shell system. The Brillouin zone integration was performed using a grid of 2 × 2 × 1 Monkhorst−Pack special *k*-points. Structure optimization was carried out using the conjugate gradient algorithm. Atoms in the top two layers of the α-Al_2O_3(0001) surface as well as the Pt clusters or monolayer were fully optimized. Atoms in the middle two layers of the slab were allowed to relax only along the direction normal to the surface, and the bottom two layers were kept fixed. The adhesion energy of the clusters on the substrate was calculated using the following expression:

$$E_{\text{adhesion}} = -(E_{\text{Pt}_n+\text{substrate}} - E_{\text{substrate}} - E_{\text{Pt}_n})/m \qquad (1)$$

where $E_{\text{Pt}_n+\text{substrate}}$ and $E_{\text{substrate}}$ are the total energies of the substrate with and without Pt_n clusters and E_{Pt_n} is the total energy of the Pt_n clusters. Here, m is the number of atoms in the Pt_n cluster in direct contact with the surface. With this definition, the adhesion energy accounts for only the cluster−substrate interface interaction. Alternatively, we can also define the adsorption energy in terms of the average of all cluster atoms

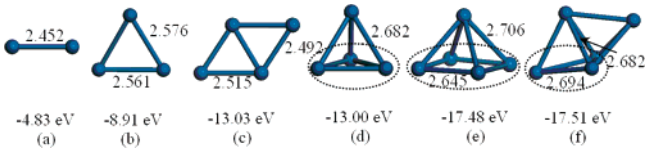

Figure 2. Geometric structures and energies of isolated Pt_n clusters ($n = 2-5$). The main bond lengths are labeled on the corresponding bonds. For three-dimensional clusters, the planes in the dashed ellipse are placed in direct contact with the surface initially.

ainvolved regardless of whether the cluster atoms are in direct contact with the substrate:

$$E_{\text{adsorption}} = -(E_{\text{Pt}_n+\text{substrate}} - E_{\text{substrate}} - E_{\text{Pt}_n})/n \qquad (2)$$

To differentiate the two definitions, we name the energy defined by eq 2 as the adsorption energy. Obviously, the magnitude of both adhesion energy E_{adhesion} and adsorption energy $E_{\text{adsorption}}$ depends on how the energy of the clusters is referenced. Several studies made use of the cohesive energy of bulk platinum to estimate the adsorption energy.[16,25] However, to be consistent, we use the calculated gas-phase Pt_n cluster energy E_{Pt_n} rather than nE_{cohesive} (including $n = 1$) as the reference, where E_{cohesive} is the Pt cohesive energy per atom. In the case of platinum monolayer, we use the average cohesive energy of the pure monolayer to evaluate the adhesion energy. The selected Pt_n clusters were first fully optimized to obtain the gas-phase energies and structures. Subsequently, the clusters were placed on the α-Al_2O_3 substrate and structural optimization was performed.

The calculations of gas-phase clusters were done by placing the clusters in a sufficiently large box to prevent interaction between clusters. The optimized cluster structures are shown in Figure 2, where the main bond distances and energy are also given. The average binding energy per atom of the cluster is calculated using the expression $E_b = E_{\text{Pt}} - E_{\text{Pt}_n}/n$, where E_{Pt} is the energy of the isolated Pt atom. Using the value of $E_{\text{Pt}} = -0.54$ eV from our calculations and the values of E_{Pt_n} given in Figure 2, we obtain $E_b = 1.88$, 2.43, 2.72, 2.71, 2.96, and 2.96 eV for structures a, b, c, d, e, and f in Figure 2, in close agreement with the values of 1.76, 2.33, 2.62, 2.68, 2.89, and 2.91 eV for structures a−f reported by Xiao and Wang.[34] Our results are also in close agreement with the results of Huda et al.[46] To further test the accuracy of the computational method, we calculated the cohesive energy of platinum, which yielded −5.88 eV per atom, in excellent agreement with the experimental value of −5.84 eV.[47] The calculated α-$Al_2O_3(0001)$ surface structure agrees well with the reported literature results.[16,21,37−39]

III. Results and Disscussion

The adsorption of Pt_n clusters on the α-$Al_2O_3(0001)$ surface was studied systematically. The results are summarized in Table 1 and discussed in detail in the following.

We first investigated the adsorption of a single Pt atom at the three possible sites shown in Figure 1a. The optimized structures and the calculated Pt−O distance distribution are shown in Figure 3. At the Al_T site, the Pt atom resides at the 3-fold hollow formed by the top layer O atoms but above the Al atom of the second layer. Three Pt−O bonds are formed with distances of approximately 1.980 Å. The calculated distance between the Pt atom and the Al atom underneath is 2.415 Å. The calculated electron density is shown in Figure 4a. Significant electron density around the Pt−O bonds is readily visible. As expected, higher electron density is around the O atoms, indicating charge flows from the Pt atom to the O atoms nearby, and consequently the Pt atom is positively charged.

At the O_{3h} site, the Pt atom is placed above the O atom in the third layer and is surrounded by four O atoms in the top layer. Structural optimization yielded four Pt−O bonds between the Pt atom and the four neighboring O atoms in the first layer, as shown in Figure 3b. In addition, although no bond was formed, the calculated distance between the Pt atom and the underneath O atom in the third layer is 3.045 Å. Of the four Pt−O bonds, one is considerably shorter than the ones at the Al_T site and two are comparable to them. The fourth bond with a distance of approximately 2.068 Å provides additional stability for the adsorption of the Pt atom. The calculated electron density shown in Figure 4b clearly indicates significant electron density around the four Pt−O bonds with higher density toward the O atoms, suggesting that the Pt atom loses charge to the O atoms.

At the O_{3v} site, the Pt atom was initially placed at the center of the 3-fold hollow above the Al atom in the second year. The subsequent geometry optimization resulted in shifting nearly horizontally the Pt atom from the center of 3-fold hollow site toward the O_{3h} site. The resulting optimized geometry is given in Figure 3c. Indeed, the optimized structure is nearly identical to the structure at O_{3h}. The calculated adhesion energy is also similar to the value for adsorption at the O_{3h} site. We therefore conclude that adsorption at the O_{3v} site is equivalent to one at the O_{3h} site.

Of the three adsorption sites, Pt atom adhesion at the Al_T site is the weakest. Using the gas-phase energy of Pt atom as the reference state, the calculated adhesion energy is 7.26 eV. Platinum binding at the O_{3h} site is much stronger with the calculated adhesion energy of 13.01 eV. It is worth noting that the calculated adhesion energies at these adsorption sites are much larger than those reported in previous calculations.[16] This should not be surprising because the values of the adhesion

TABLE 1: Energetics and Magnetic Properties of Pt−Alumina System

	adsorption site			
		adhesion energy (eV)	adsorption energy (eV)	magnetization
Pt_1	Al_T	7.26	7.26	4.511
	O_{3h}	13.01	13.01	2.997
	O_{3v}	13.01	13.01	2.901
Pt_2	Al_T-Al_T	5.53	5.53	0.666
	O_3-O_3	9.08	9.08	−0.270
Pt_3	equilateral triangle	4.27	4.27	3.022
Pt_4	planar	3.99	3.99	−0.088
	tetrahedron	4.52	3.39	−0.440
Pt_5	square pyramid	3.90	3.12	−1.837
	triangular bipyramid	4.95	2.97	4.040
Pt_{12}	monolayer	1.40	1.40	0.094
	tetrahedron film	3.73	2.80	0.670

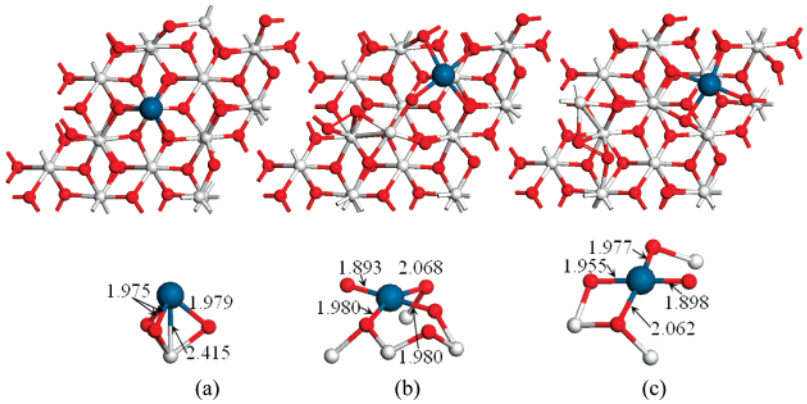

Figure 3. Local bonding of a Pt atom absorbed on selected adsorption sites: (a) Al_T site; (b) O_{3h} site; (c) O_{3v} site.

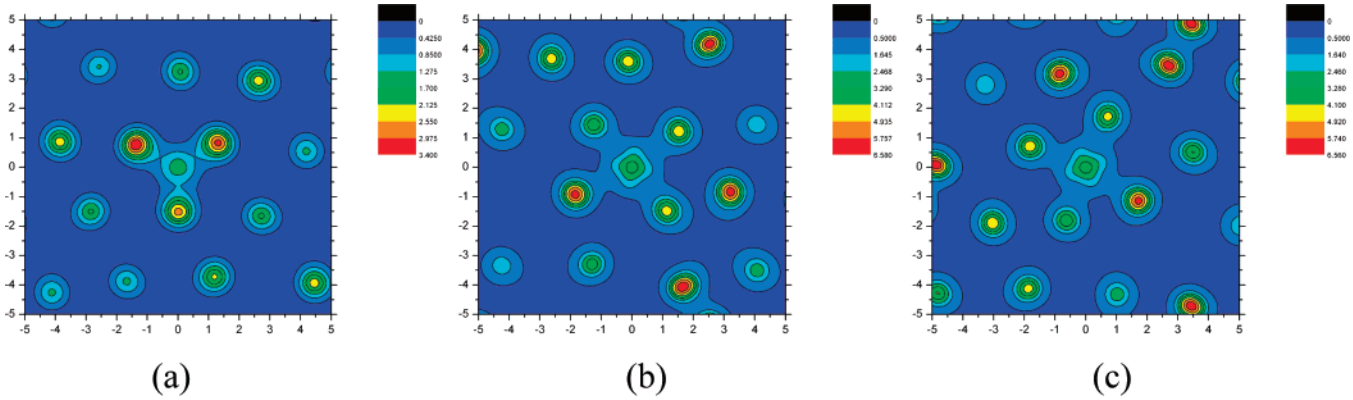

Figure 4. Electron density map of single Pt atom deposited on α-Al_2O_3(0001) reconstructed surface.

TABLE 2: Comparison of Adhesion Energies of Pt Atom on α-Al_2O_3 from the Present Work and Literature Data[16]

adsorption site	calcd adsorption energy[a] (eV)	reported adsorption energy[b] (eV)
Al_T	−1.96	−1.92
O_{3h}/O_{3v}	−7.70	−8.20

[a] This work. [b] Reference 16.

energies are sensitive to the reference energy of Pt atom used. If we were to use the cohesive energy of platinum as the reference state for the energy of Pt atom, our results would be in good agreement with the reported values by Yourdshahyan et al.[16] A comparison of the adhesion energies from the present calculation and literature data is shown in Table 2, in which the cohesive energy of Pt is used for the reference energy. For a consistent comparison with adsorption of other Pt_n clusters, from now on we use the gas-phase cluster energies to evaluate the adhesion energies.

The significantly higher adhesion energy at the O_{3h} site is largely attributed to the fact that the charge transfer from the Pt atom to the O atoms makes the Pt atom positively charged. At the Al_T site, the Al atom underneath the Pt atom is also positively charged. The repulsion between the two positively charged atoms, Pt and Al, leads to much weaker binding at this site. At the O_{3h} site, however, the Pt atom forms four bonds with the top layer O atoms. This combined with the relatively weaker attractive interaction with the underneath O atom in the third layer makes the adsorption substantially stronger. The reason adsorption at the O_{3h} site is more stable than adsorption at the O_{3v} site is that at the O_{3h} site the Pt atom interacts not only with the four O atoms on the top layer but also with the O atom underneath the third layer, while at the O_{3v} site the position beneath the Pt atom in the third layer is vacant. The Pt atom originally placed at the O_{3v} site can readily "slip" into the adjacent O_{3h} site upon structural optimization to take advantage of the additional stability provided by the O atom of the third layer. Indeed, the calculated electron density maps (Figure 4b,c) exhibit large electron densities between the Pt atom and the neighboring O atoms, indicative of strong bonding between Pt and O atoms.

We next examined the adsorption of a platinum dimer on the substrate. The dimer can be adsorbed on the surface either vertically or horizontally. Our numerical studies indicated that the vertical configuration is much less stable because the cluster cannot take full advantage of surface binding. For the horizontal configuration, two adsorption structures were obtained. First, the dimer was placed on top of two adjacent Al_T-Al_T sites with an initial separation of 2.452 Å (the gas-phase Pt−Pt bond length). Structural optimization results in significant bond relaxation with the dimer bond elongated by 0.271 Å. One Pt atom remains at the 3-fold hollow site, and another is pulled out from the adjacent Al_T site to maintain a much relaxed dimer structure. Consequently, there are only five Pt−O bonds that range from 1.915 to 2.091 Å, as shown in Figure 5a. The calculated average adhesion energy per atom is 5.53 eV, significantly smaller than the single atom adsorption. The much reduced adhesion energy arises from the fact that Pt dimer is much more stable than two separated Pt atoms in the gas phase, which results in weaker adhesion of the dimer. At the proximity of two adjacent O_{3h} sites, the dimer undergoes dissociative adsorption with each Pt atom occupying an O_{3h} adsorption site, as shown in Figure 5b. The calculated average adhesion energy is 9.08 eV. Again, compared with single Pt atom adsorption at this site, the average adhesion energy is much reduced.

To get a better understanding of the bonding between Pt atoms in the cluster and the oxygen atoms of the substrate, in Figure 5c we show the distance distribution of the Pt−O bond. The

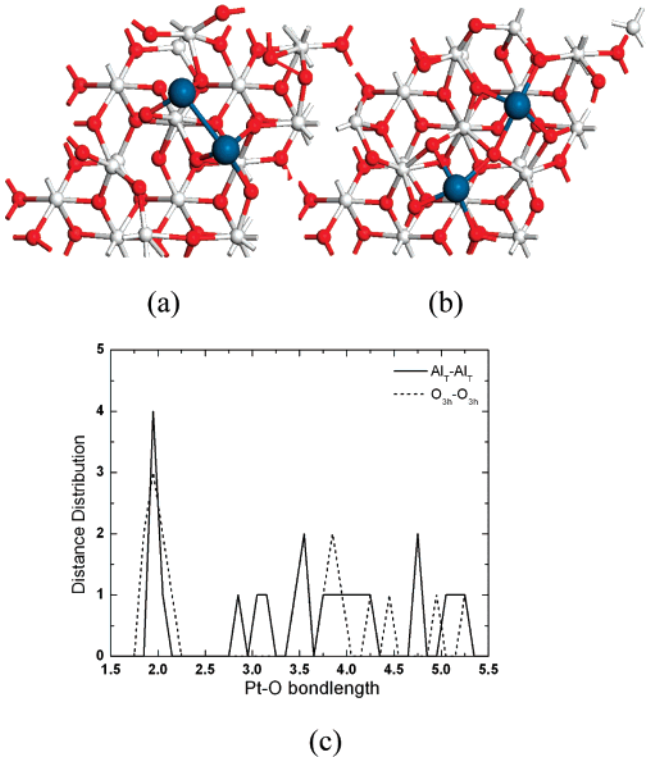

Figure 5. Pt_2 deposition: (a) Al_T-Al_T; (b) O_3-O_3. (c) Pt−O distance distribution.

distance is defined as the direct Pt−O distance between Pt atom(s) of the cluster and the oxygen atoms in the first layer. The shortest Pt−O distance in the distribution represents the bond length, while other peaks in Figure 5c describe the nonbonding Pt−O distances. It is seen that for both the Al_T-Al_T site and the $O_{3h}-O_{3h}$ site the shortest Pt−O distances are in the neighborhood of 2.0 Å.

In the remainder of the paper, we will only present results for adsorption of larger clusters at the O_{3h} site since our numerical studies suggest that adsorption at this site is much more stable than at the Al_T site. Figure 6a displays the optimized adsorption structure of a Pt_3 cluster. The cluster reorients itself parallel to the (0001) surface, forming an equilateral triangle with each Pt atom occupying an O_{3h} site. Compared with the gas-phase value, the Pt−Pt bond distance on the surface is elongated slightly by approximately 0.120 Å, indicative of the bond weakening upon interacting with the substrate. Strong Pt−O bonds are formed with bond distances ranging from 1.897 to 2.054 Å, as observed in Figure 6b, where the Pt−O distance distribution of the adsorption system is displayed. In particular, the Pt−O bonds, on average, are slightly longer than those of the smaller clusters. Significant surface relaxation occurs upon cluster adsorption. The oxygen atoms participating in the bonding with the cluster are pushed downward, while the Al atoms nearby move slightly upward. The calculated average adhesion energy is 4.26 eV, significantly lower than that of Pt and Pt_2. Nevertheless, the magnitude of the adhesion energy suggests that the cluster still remains strongly anchored on the alumina surface.

For Pt_4, we examined two energetically stable isomers: a planar rhombus and a tetrahedron. Upon structural optimization, the rhombus cluster is decomposed into an equilateral triangle and an isolated atom, as shown in Figure 7a. The equilateral triangle occupies three O_{3h} sites with a structure nearly the same as the one for Pt_3. The Pt−Pt bond distances range from 2.533 to 2.728 Å, considerably elongated from the gas-phase values

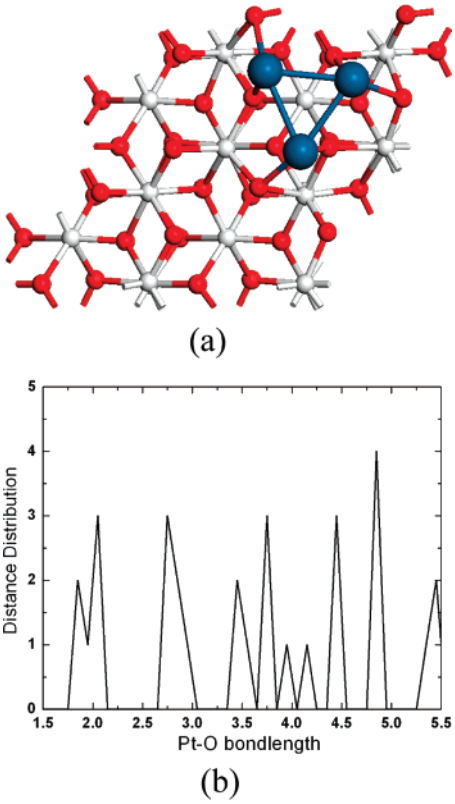

Figure 6. (a) Pt_3 equilateral triangle adsorption structure. (b) Pt−O distance distribution.

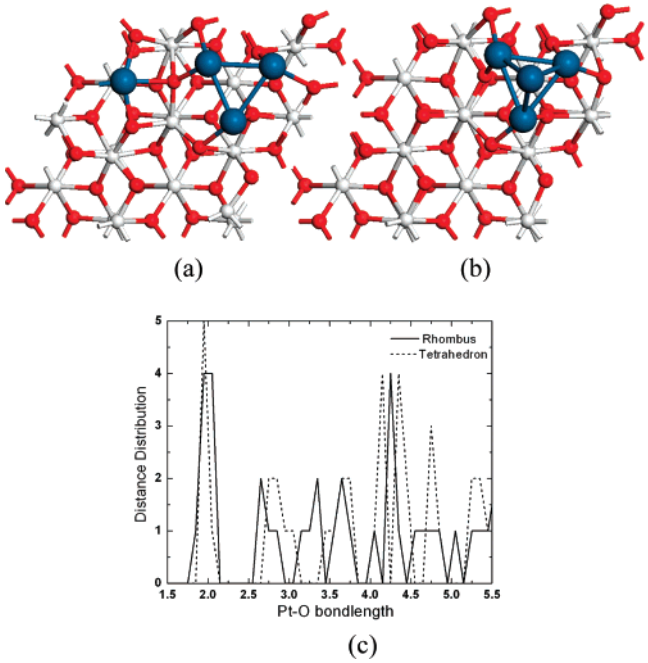

Figure 7. Pt_4 adsorption configurations: (a) planar; (b) tetrahedron. (c) Pt−O distance distribution.

by about 0.2 Å. The isolated Pt atom, originally above the Al_T site, is now displaced to a neighboring O_{3h} site, forming four Pt−O bonds with the surrounding O atoms with bond lengths of 1.906, 1.923, 1.962, and 2.061 Å. The calculated average adhesion and adsorption energies for the rhombus cluster are the same (3.99 eV), slightly lower than that of the Pt_3 cluster on the substrate, since all Pt atoms are in direct contact with the substrate. For the Pt_4 cluster with a tetrahedral geometry, the structure is slightly distorted upon geometry optimization

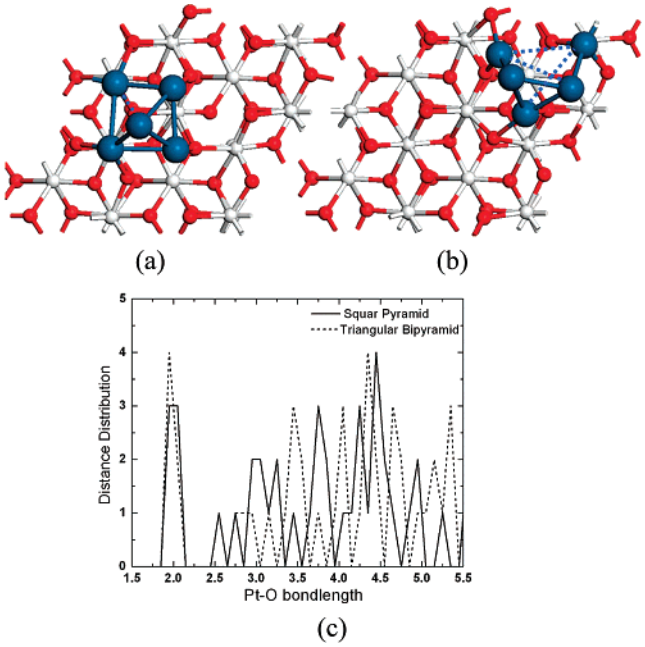

Figure 8. Pt_5 adsorption: (a) square pyramid; (b) triangular bipyramid; (c) Pt−O distance distribution.

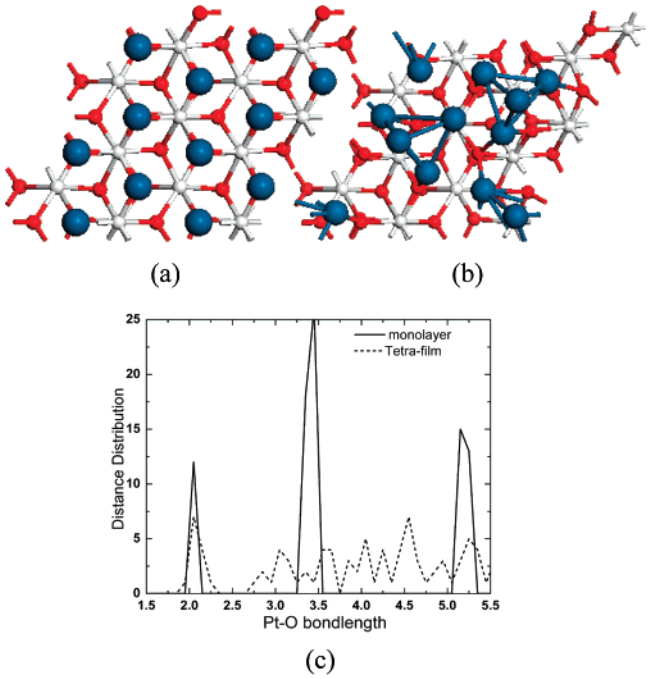

Figure 9. Adsorption of (a) Pt monolayer and (b) tetrahedron film. (c) Pt−O distance distribution.

(Figure 7b). The cluster resides above three adjacent O_{3h} sites similar to the adsorption configuration of Pt_3, except that the fourth atom is on top of the triangle. The bond lengths between the top Pt atom and the bottom three Pt atoms are approximately 2.627 Å, slightly shorter than the gas-phase value of 2.686 Å,[36] indicating higher bond strength. The calculated average adhesion energy is 4.52 eV, slightly higher than that of the Pt_3 cluster, which is attributed mostly to the smaller number of Pt atoms in direct contact with the substrate. In contrast, the calculated average adsorption energy (3.39 eV) in this case is smaller than that of Pt_3 because it also accounts for the top Pt atom that is not in direct contact with the surface. It is worth noting from Figure 7c that the Pt atoms of the tetrahedron structure directly interacting with the substrate have slightly smaller Pt−O bond lengths than those of the rhombus cluster, consistent with the calculated adhesion energies. In both cases, the Pt−O bond distances are elongated slightly compared with those observed in smaller clusters, suggesting weaker cluster−substrate bonding.

For Pt_5, we consider adsorption of two isomers with comparable binding energies, triangular bipyramid and square pyramid. In the gas phase, the triangular bipyramid structure is slightly more stable than the square pyramid structure by 0.03 eV. Upon adsorption on the substrate, the square pyramid cluster becomes distorted with one Pt atom at the bottom shifted to an adjacent O_{3h} site forming three Pt−O bonds with bond distances ranging from 1.913 to 1.990 Å. The other four Pt atoms adopt a distorted triangular pyramid structure on the surface (Figure 8a). The calculated average adhesion and adsorption energies are 3.90 and 3.12 eV, respectively, further declining from those of the Pt_4 cluster. Nevertheless, the adhesion of this cluster to the substrate is still rather strong. For adsorption of the triangular bipyramid geometry, we observed significant structural relaxation with one triangular face, highlighted in Figure 2f, interacting with the substrate directly and another atom coming off the cluster to reside in a nearby O_3 site. Consequently, the triangular bipyramid structure is pulled apart and partially dissociated, leading to a stronger adhesion of the cluster on the surface (Figure 8b). Indeed, the calculated adhesion energy of 4.95 eV is about 1.0 eV higher than that of the square pyramid structure. The computed Pt−O distance distributions (Figure 8c) clearly indicate that the bond distance between Pt and O located around 2.0 Å is slightly shorter for the triangular bipyramid than for the square pyramid. However, on average, the bonds are elongated compared to those of smaller clusters, indicating weaker adhesion on the substrate.

An interesting issue on Pt loading on the α-Al_2O_3(0001) substrate is whether Pt atoms prefer wetting or clustering upon adsorption. To address this issue, we investigated adhesion of a Pt monolayer and three islands of Pt_4 tetrahedral clusters on the substrate shown in Figure 9a,b. For the monolayer, all atoms, originally placed at the O_3 hollow sites, now shift to the on-top sites of O atoms upon energy minimization with a Pt−O bond distance of 2.011 Å. This should not be surprising because each O atom interacts with a Pt atom in this case regardless of where the Pt atom is located. At the O_3 site, the bonding between the Pt atom and the neighboring three O atoms is not as effective as the one at the on-top site due to the structural constraint of the substrate. The on-top mode allows the Pt atoms to maximally approach the O atoms. To examine whether agglomeration could occur from the Pt monolayer, we placed three tetrahedral Pt_4 clusters on the substrate. We found that while stable adsorption structure was formed upon structural optimization the tetrahedral configurations are somewhat distorted, as shown in Figure 9b. The calculated Pt−O distance distribution is displayed in Figure 9c. While for the perfectly aligned monolayer structure distinct Pt−O distances are clearly visible, for the Pt_4 clusters the distance appears to spread out with the Pt−O bond lengths centered around 2.10 Å but with fewer Pt−O bonds than in the case of the monolayer. The Pt−Pt bonds are essentially dissociated with an average distance of 2.77 Å in the case of the monolayer, indicating weak metallic interaction. In the case of cluster film, the calculated Pt−Pt bond distance ranges from 2.639 to 2.847 Å within a cluster. The calculated adhesion energy and adsorption energy for the Pt monolayer are the same, 1.40 eV. However, for the cluster film, these quantities are much higher (3.73 and 2.79 eV, respectively), indicating a strong preference for clustering over wetting. The stronger adsorption of the clusters arises from the greater Pt−Pt bonding than Pt−O bonding, and the higher adhesion energy reflects the fact that

fewer Pt atoms are in direct contact with the substrate. The results suggest that Pt loading on α-Al_2O_3(0001) surface would unlikely undergo a smooth deposition pathway and agglomeration could occur upon cluster adsorption on the substrate. This can be advantageous for catalysis since the metal clustering could give rise to more sharp corners for catalytic reactions. However, metal agglomeration could also lead to shrinkage of catalyst surface area.

In general, Pt clusters contain unpaired electrons in their d orbitals and thus are magnetic. Upon adsorption on α-Al_2O_3-(0001) substrate, considerable change in their electronic states can take place. Indeed, the calculated density of states (DOS), depicted in Figure 10, show substantial feature changes. For the substrate alone (Figure 10, top), the symmetric DOS spectrum shows typical features of a closed-shell system. Upon Pt cluster loading, some of the low-lying states are unevenly populated, resulting in magnetic moments in the supported clusters. The valence bands are considerably expanded with the Pt atoms transferring charges to the O atoms of the substrate. As a consequence, the unoccupied 2p orbitals of the O atoms are now underneath the Fermi level, while part of the Pt 5d bands is pushed above the Fermi level. It is worth noting, in particular, that for the monolayer the calculated DOS spectrum exhibits perfect symmetric features, indicating a closed-shell system with a band gap roughly of 0.8 eV, while for the cluster film the DOS spectrum suggests a magnetic system with no observed band gap. The strong overlap between the valence band and the conduction band suggests that the cluster film could be catalytically more active.

IV. Summary

Oxide supported precious metals play an important role in many heterogeneous catalytic reactions. Understanding of the interactions between the support materials and the metal particles is of fundamental importance for the development of efficient catalytic systems for a wide variety of applications. In the present paper, we attempt to address some of the fundamental aspects of these interactions by examining the adhesion of small Pt_n clusters on the α-Al_2O_3(0001) surface using density functional theory. The results provide useful physical insights into the adhesion forces that lead to the anchoring of the metal clusters.

We first carefully defined adsorption energy based on the relative average adsorption strength and adhesion energy according to the direct contact of cluster atoms with the substrate. We then identified energetically the most favorable adsorption sites for small Pt_n clusters up to $n = 5$ and found that the O_3 site is strongly preferred. Substantial structural relaxation of the clusters occurs upon placing them on the substrate followed by energy minimization. In general, the extent of structural distortion decreases as the cluster size increases. In particular, we found that for clusters larger than $n = 3$ the cluster prefers to interact with the substrate via its triangular face to take advantage of the maximum interaction with the available O_3 sites. Both the calculated adhesion and adsorption energies decline with the cluster size, consistent with the increasingly elongated average Pt−O bond distances. Nevertheless, in all cases, we found that the clusters can be stably anchored on the surface. The driving force of the cluster anchoring largely arises from the charge transfer from Pt atoms to the O atoms of the substrate.

We have also attempted to address whether clusters would undergo agglomeration or wetting upon adsorption by examining adsorption of a monolayer and cluster islands on the surface.

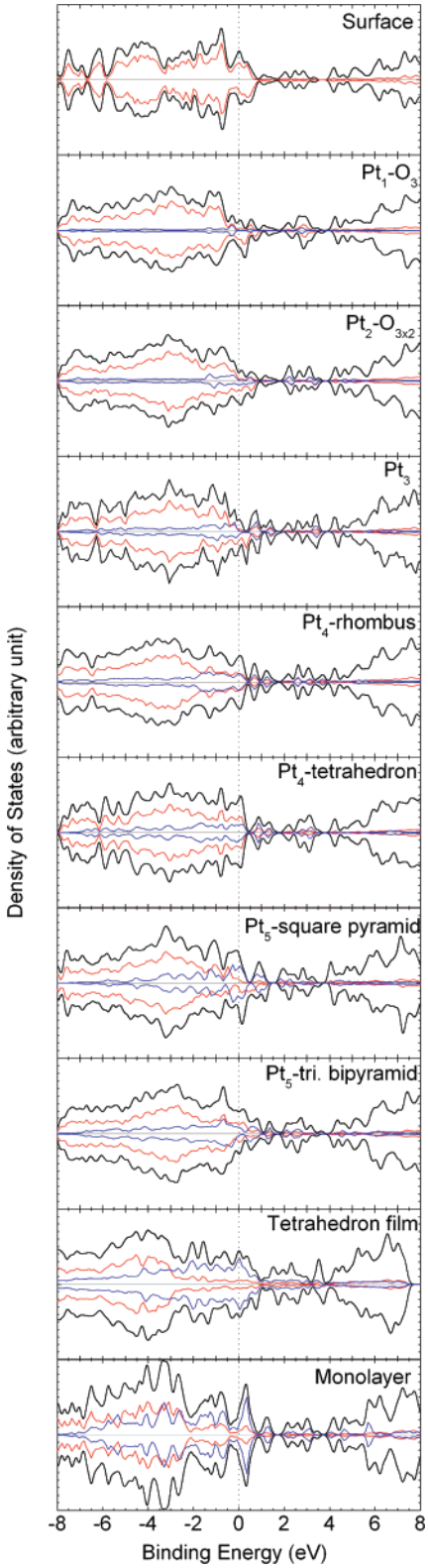

Figure 10. Density of states of the catalyst−support system. The black bold lines represent the total DOS, the red lines are the contribution of O atoms, and the blue lines are that of Pt atoms.

We found that energetically metal clustering is strongly preferred due to the strong Pt−Pt bonding. The cluster islands exhibit sharp corners, giving rise to higher reactivity toward gas-phase molecules; however, they could also potentially reduce the surface sites at the same time. The structure of the supported Pt cluster film could serve as an useful model to study chemical reactions. Our results indicate that growth of metal films on

the α-Al_2O_3 surface is unlikely to be smooth and agglomeration could occur under certain conditions. However, it still remains unclear how high the energy barrier associated with the structural transition is, which we plan to investigate in future work.

Acknowledgment. This work was supported by DOE Grant DE-FG36-05GO85028. C.Z. acknowledges partial support from the Research Foundation for Outstanding Young Teachers, China University of Geosciences, Wuhan (Grant CUGQNL0519). We thank Philippe Weck, Eunja Kim, P. Tarakeshwar, and Clemens Heske for many useful discussions and consultations. Thanks are also due to Dr. Andrew M. Rappe and Dr. Valentino R. Cooper for providing the α-Al_2O_3(0001) surface structures.

References and Notes

(1) Verdozzi, C.; Jennison, D. R.; Schultz, P. A.; Sears, M. P. *Phys. Rev. Lett.* **1999**, *82*, 799.
(2) Gomes, J. R. B.; Illas, F.; Hernádez, N. C.; Máquez, A.; Sanz, J. F. *Phys. Rev. B* **2002**, *65*, 125414.
(3) Carrey, J.; Maurice, J. L.; Petroff, F.; Vaures, A. *Surf. Sci.* **2002**, *504*, 75.
(4) Molina, L. M.; Hammer, B. *Phys. Rev. Lett.* **2003**, *90*, 206102.
(5) Gao, H.; He, H.; Feng, Q.; Wang, J. *Spectrochim. Acta, Part A: Mol. Biomol. Spectrosc.* **2005**, *61*, 3117.
(6) Tzitzios, V. K.; Georgakilas, V. *Chemosphere* **2005**, *59*, 887.
(7) Benam, M. R.; Aliabad, H. A. R.; Hosseini, S. M. *Phys. Status Solidi A* **2006**, *203*, 2223.
(8) Comotti, M.; Li, W. C.; Spliethoff, B.; Schuth, F. *J. Am. Chem. Soc.* **2006**, *128*, 917.
(9) Wu, Q.; Gao, H.; He, H. *J. Phys. Chem. B* **2006**, *110*, 8320.
(10) Montano, M.; Bratlie, K.; Salmeron, M.; Somorjai, G. A. *J. Am. Chem. Soc.* **2006**, *128*, 13229.
(11) Palazov, A.; Bonev, C.; Shopov, D.; Lietz, G.; Sárkány, A.; Völter, J. *J. Catal.* **1987**, *103*, 249.
(12) Altman, E. I.; Gorte, R. J. *J. Phys. Chem.* **1989**, *93*, 1993.
(13) Hensley, D. A.; Kesmodel, L. L. *J. Phys. Chem.* **1991**, *95*, 1368.
(14) Asakura, K.; Tomishige, K.; Shirai, M.; Chun, W. J.; Yokoyama, T.; Iwasawa, Y. *Physica B* **1995**, *208*, 637.
(15) Putna, E. S.; Vohs, J. M.; Gorte, R. J. *Surf. Sci.* **1997**, *391*, L1178.
(16) Yourdshahyan, Y.; Cooper, V. R.; Kolpak, A. M.; Rappe, A. M. *Proc. SPIE* **2003**, *5223*, 223.
(17) DeJong, V.; Cieplik, M. K.; Louw, R. *Environ. Sci. Technol.* **2004**, *38*, 5217.
(18) Gonzalez-Marcos, M. P.; Inarra, B.; Guil, J. M.; Gutierrez-Ortiz, M. A. *Appl. Catal., A* **2004**, *273*, 259.
(19) Szyja, B.; Szczygieł, J.; Tymków, I. *J. Mol. Model.* **2005**, *11*, 370.
(20) Alexeev, O. S.; Li, F.; Amiridis, M. D.; Gates, B. C. *J. Phys. Chem. B* **2005**, *109*, 2338.
(21) Cooper, V. R.; Kolpak, A. M.; Yourdshahyan, Y.; Rappe, A. M. *Phys. Rev. B* **2005**, *72*, 081409.
(22) Gonzalez-Marcos, M. P.; Inarra, B.; Guil, J. M.; Gutierrez-Ortiz, M. A. *Catal. Today* **2005**, *107*−*108*, 685.
(23) Alexeev, O. S.; Siani, A.; Lafaye, G.; Williams, C. T.; Ploehn, H. J.; Amiridis, M. D. *J. Phys. Chem. B* **2006**, *110*, 24903.
(24) Atalik, B.; Uner, D. *J. Catal.* **2006**, *241*, 268.
(25) Ishimoto, R.; Jung, C. H.; Tsuboi, H.; Koyama, M.; Endou, A.; Kubo, M.; Del Carpio, C. A.; Miyamoto, A. *Appl. Catal., A* **2006**, *305*, 64.
(26) Minemura, Y.; Kuriyama, M.; Ito, S.; Tomishige, K.; Kunimori, K. *Catal. Commun.* **2006**, *7*, 623.
(27) Wootsch, A.; Paal, Z; Gyorffy, N.; Ello, S.; Boghian, I.; Leverd, J.; Pirault-Roy, L. *J. Catal.* **2006**, *238*, 67.
(28) Baxter, R.; Reinhardt, P.; López, N.; Illas, F. *Surf. Sci.* **2000**, *445*, 448.
(29) Wander, A.; Searle, B.; Harrison, N. M. *Surf. Sci.* **2000**, *458*, 25.
(30) Sartale, S. D.; Shiu, H. W.; Ten, M. H.; Huang, J. Y.; Luo, M. F. *Surf. Sci.* **2006**, *600*, 4978.
(31) Zhang, W.; Zhao, H.; Wang, L. *J. Phys. Chem. B* **2004**, *108*, 2140.
(32) Knickelbein, M. B. *Annu. Rev. Phys. Chem.* **1999**, *50*, 79.
(33) Dai, D.; Balasubramanian, K. *J. Chem. Phys.* **1995**, *103*, 648.
(34) Xiao, L.; Wang, L. *J. Phys. Chem. A* **2004**, *108*, 8605.
(35) Xiao, L.; Wang, L. *J. Phys. Chem. C* **2007**, *111*, 1657.
(36) Nie, A.; Wu, J.; Zhou, C.; Yao, S.; Luo, C.; Forrey, R. C.; Cheng, H. *Int. J. Quantum Chem.* **2007**, *107*, 219.
(37) Knozinger, H.; Ratnasamy, P. *Catal. Rev. Sci.* **1978**, *17*, 31.
(38) Tsyganenko, A. A.; Mardilovich, P. P. *J. Chem. Soc., Faraday Trans.* **1996**, *92*, 4843.
(39) Hass, K. C.; Schneider, W. F.; Curioni, A.; Andreoni, W. *Science* **1998**, *282*, 265.
(40) Kresse, G.; Hafner, J. *Phys. Rev. B* **1993**, *47*, 558.
(41) Kresse, G,; Hafner, J. *Phys. Rev. B* **1994**, *49*, 14251.
(42) Kresse, G.; Furthmüller, J. *Phys. Rev. B* **1996**, *54*, 11169.
(43) Kresse, G.; Furthmüller, J. J. *Comput. Mater. Sci.* **1996**, *6*, 15.
(44) Blöchl, P. E. *Phys. Rev. B* **1994**, *50*, 17953.
(45) Kresse, G.; Joubert, D. *Phys. Rev. B* **1999**, *59*, 1758.
(46) Huda, M. N.; Niranjan, M. K.; Sahu, B. R.; Kleinman, L. *Phys. Rev. A* **2006**, *73*, 053201.
(47) Kittel, C. In *Introduction to Solid State Physics*, 7th ed.; Wiley: New York, 1996.